

# Metastatic Ovarian and Primary Peritoneal Cancer: Assessing Chemotherapy Response with Diffusion-weighted MR Imaging—Value of Histogram Analysis of Apparent Diffusion Coefficients<sup>1</sup>

Stavroula Kyriazi, MD  
David J. Collins, BA  
Christina Messiou, MD  
Kjell Pennert, BSc  
Robert L. Davidson, MRRes  
Sharon L. Giles, BSc  
Stan B. Kaye, FRCP, FMedSci  
Nandita M. deSouza, MD, FRCR

<sup>1</sup>From the Cancer Research-UK and EPSRC Cancer Imaging Centre (S.K., D.J.C., C.M., R.L.D., S.L.G., N.M.d.S.), Research Data Management and Statistics Unit (K.P.), and Department of Gynaecological Oncology (S.B.K.), Royal Marsden NHS Foundation Trust and Institute of Cancer Research, Downs Road, Sutton, Surrey SM2 5PT, England. Received March 19, 2011; revision requested May 1; revision received May 24; accepted June 7; final version accepted June 14. Supported by EC FP6 Marie Curie Action, Molecular Imaging for Translational Research Applications in Cancer (contract 020718), Cancer Research UK and EPSRC Cancer Imaging Centre in association with Medical Research Council and Department of Health (England; grant C1060/A103334), and National Health Service funding to National Institute for Health Research Biomedical Research. Address correspondence to S.K. (e-mail: [Stavroula.Kyriazi@icr.ac.uk](mailto:Stavroula.Kyriazi@icr.ac.uk)).

© RSNA, 2011

## Purpose:

To prospectively evaluate apparent diffusion coefficient (ADC) histograms in the prediction of chemotherapy response in patients with metastatic ovarian or primary peritoneal cancer.

## Materials and Methods:

Research ethics committee approval and patient written informed consent were obtained. Diffusion-weighted (DW) magnetic resonance (MR) imaging was performed through the abdomen and pelvis before and after one and three cycles of chemotherapy in 42 women (mean age, 63.0 years  $\pm$  11.4 [standard deviation]) with newly diagnosed or recurrent disease. Reproducibility and intra- and interobserver agreement of ADC calculations were assessed. Per-patient weighted ADC histograms were generated at each time point from pixel ADCs from five or fewer target lesions. Mean ADC, percentiles (10th, 25th, 50th, 75th, 90th), skew, kurtosis, and their change were analyzed according to histologic grade, primary versus recurrent disease status, and response, determined with integrated biochemical and morphologic criteria, with a linear mixed model. Areas under receiver operating characteristic curve (AUCs) for combinations of parameters were calculated with linear discriminant analysis.

## Results:

Coefficients of variation for repeat measurements and for within and between observers were 4.8%, 11.4%, and 13.7%, respectively. Grade and disease status did not significantly affect histogram parameters. Pretreatment ADCs were not predictive of response. In responders, all ADCs increased after the first and third cycle ( $P < .001$ ), while skew and kurtosis decreased after the third ( $P < .001$  and  $P = .006$ , respectively); however, in nonresponders, no parameter changed significantly. Percentage change of the 25th percentile performed best in identifying response (AUC = 0.82 and 0.83 after first and third cycle, respectively), whereas combination of parameters did not improve accuracy.

## Conclusion:

An early increase of ADCs and later decrease of skew and kurtosis characterize chemotherapy response. Quantitative DW MR imaging can aid in early monitoring of treatment efficacy in patients with advanced ovarian cancer.

© RSNA, 2011

**E**pithelial ovarian cancer is the most lethal gynecologic malignancy because of its often metastatic stage at presentation and the almost inevitable development of resistance to various chemotherapeutic agents during the course of disease (1). Although response to primary chemotherapy with a platinum-taxane combination is 70%–80% (2), most patients relapse after a median progression-free interval of 18 months and achieve increasingly poorer response rates to second- or third-line regimens (3). In these patients, individualized prediction of chemosensitivity would be highly desirable to avoid toxicity of inefficient agents. Monitoring response to chemotherapy currently relies on biochemical (serum CA-125 level) and imaging (size reduction) criteria, the combination of which

describes global clinical response after completion of treatment. However, the predictive value of these biomarkers is limited, and the magnitude of change required to signify response is rarely attained early in the course of treatment, thus failing to facilitate a timely change of clinical treatment in nonresponders (4,5).

Diffusion-weighted (DW) magnetic resonance (MR) imaging is a functional technique that develops image contrast through the inhibitory effect of cell membranes on the mobility of water molecules in tissues. As a result of their dense cellularity, malignant lesions have restricted diffusion, which is reflected in their low mean apparent diffusion coefficients (ADCs). This parameter has been used to characterize tumors and quantify treatment-induced changes, which may occur earlier than conventional morphologic alterations (6–8). In addition to the use of an average ADC, histogram analysis of ADCs can interrogate the biologic heterogeneity of tumor by classifying domains of different diffusivity, which may have prognostic and predictive implications (9,10).

In advanced ovarian cancer, qualitative DW MR imaging has been shown to improve staging accuracy by enhancing the detectability of peritoneal implants (11), while the feasibility of quantitative DW MR imaging in multiple sites of disease, including primary ovarian and metastatic peritoneal or omental, has been reported (12). However, the use of ADC histograms as a surrogate marker of chemotherapy response has not, to our knowledge, been explored yet. We hypothesized that the pattern of ADC change may differ between responding and nonresponding patients.

#### Implication for Patient Care

- In patients with metastatic ovarian or primary peritoneal cancer, diffusion-weighted MR imaging has potential for monitoring treatment efficacy, because changes on ADC histograms correlate with and often precede size and tumor-marker evidence of response.

The purpose of this study, therefore, was to investigate the value of ADC histogram analysis in the assessment of chemotherapy response in patients with metastatic ovarian cancer.

#### Materials and Methods


##### Patients

This prospective single-institution study was local research ethics committee approved. All patients participating gave written informed consent. During a 22-month period (November 2008 to September 2010), 59 consecutive female patients were recruited. The inclusion criteria were (a) histopathologic diagnosis of primary ovarian or peritoneal cancer, either newly diagnosed or recurrent; (b) presence of a minimum of one peritoneal or omental lesion, measuring at least 10 mm in maximum diameter at computed tomography (CT) or MR imaging; (c) being scheduled to receive platinum- or taxane-based chemotherapy; and (d) no contraindications to MR imaging. Inclusion of both newly diagnosed and recurrent disease in patients ensured that sufficient numbers of responders and nonresponders would be available for analysis, because response rates vary remarkably

#### Advances in Knowledge

- In patients with metastatic ovarian or primary peritoneal cancer with CA-125 level and Response Evaluation Criteria in Solid Tumors response, a significant increase of mean and percentile apparent diffusion coefficients (ADCs) is seen on histograms of whole tumor burden after the first cycle of chemotherapy, with a decrease of ADC histogram skew and kurtosis after the third cycle.
- Responders had a greater change in all ADC histogram parameters after the first and third cycle than nonresponders, with changes of the 25th ADC percentile being most discriminatory at both time points.
- After the first cycle of chemotherapy, an increase of the 25th ADC percentile, which was greater than the 95% confidence interval of reproducibility, had an improved positive predictive value over conventional biochemical and morphologic criteria (89.8% vs 64.8%), with a similar negative predictive value (36.0% vs 35.7%).

#### Published online before print

10.1148/radiol.11110577 **Content code:** 

**Radiology** 2011; 261:182–192

#### Abbreviations:

ADC = apparent diffusion coefficient  
 AUC = area under receiver operating characteristic curve  
 DW = diffusion weighted  
 RECIST = Response Evaluation Criteria in Solid Tumors  
 ROI = region of interest

#### Author contributions:

Guarantors of integrity of entire study, S.K., N.M.d.S.; study concepts/study design or data acquisition or data analysis/interpretation, all authors; manuscript drafting or manuscript revision for important intellectual content, all authors; manuscript final version approval, all authors; literature research, S.K., D.J.C., S.L.G.; clinical studies, S.K., D.J.C., C.M., S.L.G., S.B.K., N.M.d.S.; statistical analysis, S.K., K.P., R.L.D.; and manuscript editing, S.K., D.J.C., K.P., S.L.G., S.B.K., N.M.d.S.

Potential conflicts of interest are listed at the end of this article.

between primary and recurrent disease status (13). Among these patients, we excluded those in whom lesions were not deemed evaluable with DW MR imaging results because of artifact ( $n = 7$ ), those who did not receive chemotherapy ( $n = 4$ ) or whose chemotherapy was discontinued ( $n = 1$ ), those in whom the intratreatment MR imaging study was delayed beyond 21 days after the previous cycle of chemotherapy ( $n = 2$ ), those in whom main disease burden consisted of lymphadenopathy ( $n = 1$ ), and those in whom definitive histopathologic diagnosis was different from initially presumed ovarian cancer ( $n = 2$ ). The reason for excluding the patient with primarily nodal disease was that this cohort has been associated with a different prognosis than other types of stage III ovarian cancer (14). Finally, 42 patients (mean age, 63.0 years  $\pm$  11.4 [standard deviation]; range, 34–85 years) composed the study population.

### Imaging Schedule

MR imaging was performed at baseline and after one and three cycles of a six-cycle chemotherapy scheme. In platinum-based regimens ( $n = 42$ ), the agent was administered on day 1 of a 21-day cycle. In taxane-based regimens ( $n = 3$ ), the agent was administered on days 1, 8, and 15 of a 28-day cycle. The median time interval between baseline study and start of chemotherapy was 4 days (range, 0–13 days), that between day 1 of the first cycle and the first intratreatment MR imaging was 10.5 days (range, 2–18 days), and that between day 1 of the third cycle and the second intratreatment MR imaging was 7 days (range, 1–18 days).

All MR imaging studies were performed with a 1.5-T system (Avanto; Siemens Medical Systems, Erlangen, Germany) with two six-channel phased-array body coils for anatomic coverage of the abdomen and pelvis. Antispasmodic hyoscine butylbromide (Buscopan; Boehringer, Ingelheim, Germany) (20 mg intramuscularly) was administered before image acquisition to reduce motion artifact. Morphologic imaging was performed with axial T1-weighted gradient-recalled-echo and T2-weighted

turbo spin-echo sequences. DW MR imaging was performed with an axial free-breathing single-shot echo-planar technique with parallel imaging (acceleration factor of two) and spectral adiabatic inversion-recovery fat suppression. Diffusion gradients with  $b$  values of 0, 600, 900, and 1050 sec/mm<sup>2</sup> were applied in three orthogonal directions and were averaged to provide isotropic trace images. Imaging parameters were as follows: repetition time, 6300 msec for abdomen and 7900 msec for pelvis; echo time, 69 msec for abdomen and pelvis; flip angle, 90°; number of sections, 40 for abdomen and 50 for pelvis; section thickness, 5 mm; no intersection gap; voxel volume, 3  $\times$  3  $\times$  5 mm; number of signals acquired, five; matrix, 128  $\times$  128 interpolated to 256  $\times$  256; field of view, 380 mm; and bandwidth, 1776 Hz per pixel. Average DW MR imaging acquisition time was 5 minutes 35 seconds in the abdomen and 7 minutes in the pelvis. The entire MR imaging examination lasted approximately 35 minutes.

### Lesion Evaluation and ADC Histograms

Image analysis was performed off-line by a radiologist (S.K., with 2 years of experience in body DW MR imaging) who was blinded to clinical response status. Up to five largest measurable lesions were selected in each patient. For each lesion, size (the maximum diameter measured with a caliper tool to the nearest millimeter on axial T2-weighted images) and site (peritoneal, omental, ovarian, and visceral) were recorded.

Dedicated IDL-based (Research Systems, Boulder, Colo) software (DiffusionView; Institute of Cancer Research, London, England) was used for ADC calculation, segmentation of regions of interest (ROIs), and image registration. ADC maps were generated through monoexponential fitting of signal intensity for all four  $b$  values. ROIs were grown on the  $b = 1050$  sec/mm<sup>2</sup> DW MR images with a computer-assisted interactive technique, whereby the operator positioned a seed within the lesion and defined the standard deviation of signal intensity values to be included. Cystic or necrotic areas

were excluded by visual matching with anatomic T2-weighted images. In 12 lesions (two ovarian, five peritoneal, four omental, and one visceral), ROIs were drawn manually because subtle signal intensity differences between the tumor and surrounding tissue were beyond the segmentation capacity of the software. ROIs were then registered to the corresponding ADC maps, and ADCs were recorded for each pixel. After summation of pixel ADCs from all target lesions, per-patient ADC histograms (bin width, 1  $\times$  10<sup>-6</sup> mm<sup>2</sup>/sec) were generated, in which the contribution of each individual lesion was weighted according to its volume. Histogram-derived parameters were (a) mean ADC; (b) 10th, 25th, 50th, 75th, and 90th percentiles (which indicated the pixel ADC below which the corresponding percentage of all ADCs lie); and (c) skew, or  $\gamma$ , and kurtosis, or  $K$  (measures of the asymmetry of ADC distribution). Percentage change of ADC mean and percentile points for intratreatment time point  $t$  was calculated as follows:  $\% \Delta \text{ADC}_t = [(\text{ADC}_t - \text{ADC}_0) / \text{ADC}_0] \times 100$ , where  $\text{ADC}_t$  and  $\text{ADC}_0$  were ADC parameters obtained at follow-up and baseline, respectively. Change in skew and kurtosis was defined as follows:  $\Delta \gamma_t = \gamma_t - \gamma_0$  and  $\Delta K_t = K_t - K_0$ , where  $\gamma_t$  and  $K_t$  represented skew and kurtosis at follow-up and  $\gamma_0$  and  $K_0$  represented skew and kurtosis at baseline, respectively. The width of ADC histograms was assessed as the difference between the 90th percentile and the 10th percentile to exclude outliers. Lesions in which maximal diameter decreased to less than 10 mm as a result of treatment were not deemed assessable and were withdrawn from analysis at the corresponding time point.

### Reproducibility and Intra- and Interobserver Agreement

To assess the short-term reproducibility of the technique, 10 randomly selected patients underwent repeated DW MR imaging after completion of the standard imaging protocol. Prior to repetition, the imaging table was moved, patients were dismounted and remounted, and a new imaging survey was performed.

The time interval between the two DW MR imaging acquisitions was approximately 10 minutes.

The assessment of intra- and interobserver agreement was powered according to previously reported coefficient of ADC reproducibility in abdominal organs of 14% (15). To detect a difference of this magnitude with 80% power and .05 significance level, a sample size of 54 matched lesions was calculated and randomly selected with software (SPSS, version 18.0; SPSS, Chicago, Ill). Intraobserver variability was assessed in two sessions, 15 weeks apart, by a radiologist (S.K.) who was blinded to the results of the first session with regard to shape and size of ROI and ADC measurements. For assessment of interobserver variability, ROIs were drawn with the same segmentation software in the designated lesions by a second radiologist (C.M., with 3 years of experience in body DW MR imaging) who had no access to the results of the first observer.

### Assessment of Chemotherapeutic Response

Standard treatment monitoring comprised serum CA-125 level measurements and CT imaging results before and after the third and sixth cycles of chemotherapy. Response was determined at the end of treatment with the integrated biochemical and morphologic criteria for ovarian cancer clinical trials, whereby a reduction of serum CA-125 level by more than 50% with concomitant imaging assessment other than progressive disease (including complete and partial response and stable disease) in up to five target lesions according to Response Evaluation Criteria in Solid Tumors (RECIST) are needed to classify response (16). Nonprogressive disease according to RECIST is defined as absence of new lesions and reduction of any magnitude or increase of less than 20% in the sum of maximum diameters (17). Inversely, progressive disease according to RECIST accompanied by any change in serum CA-125 level signifies lack of response (14). The same target lesions as in DW MR imaging analysis were used

for morphologic response assessment. According to guidelines, in 12 patients who underwent interval debulking surgery after three cycles of neoadjuvant chemotherapy, response assessment was undertaken after the third cycle to exclude the effect of surgical cytoreduction on disease burden (16).

### Statistical Analysis

Statistical analysis was performed with software (SPSS, version 18.0; SPSS). Reproducibility of mean ADC was assessed by applying Bland-Altman analysis (18), whereby the respective coefficients, indicating the greatest difference between replicate ADC measurements in 95% of paired observations, were calculated as  $r = 1.96 \times$  standard deviation of percentage ADC difference. Intra- and interobserver agreement were assessed with intraclass correlation coefficients (19), where an intraclass correlation coefficient greater than 0.75 was considered indicative of good agreement, and with Bland-Altman analysis (18), where the difference in paired mean ADCs was plotted against the average from the two readings. Pre- and intratreatment ADC parameters and their percentage change in responding and nonresponding patients were analyzed with a linear mixed-effects model, in which ADCs were the dependent variables, while the independent variables were subject (random factor) and primary versus recurrent disease status, tumor grade, and response (fixed factors). Spearman rank correlation coefficient was used to assess the relationship across times between change of ADC parameters and (a) percentage volume change of disease burden (inferred from cumulative pixel count of target lesions on DW MR images) and (b) percentage CA-125 level change. The subset of ADC variables that would optimally separate responders from nonresponders was investigated with leave-one-out linear discriminant analysis (20), the output of which was used to create receiver operating characteristic curves, with the area under the receiver operating characteristic curve (AUC) as a measure of diagnostic performance. In the cohort of responders,

6-month progression-free survival was analyzed with multivariate Cox regression, where age, tumor grade, absence of measurable disease and normal CA-125 level at the end of treatment, and the best ADC classifier were introduced as covariates. A two-sided *P* value less than .05 was considered to indicate a statistically significant difference in all analyses.

## Results

### Demographics

Patient characteristics, histologic diagnosis, therapeutic history, and number and site of analyzed lesions are summarized in Table 1. Among 42 patients, there were 32 (76%) responders (22 new diagnosis, 10 recurrent disease) and 10 (24%) nonresponders (one new diagnosis, nine recurrent disease). Among 23 patients with newly diagnosed disease, 12 (52%) were deemed initially inoperable and were treated with three cycles of neoadjuvant chemotherapy and interval debulking surgery, eight (35%) with measurable residual disease after primary debulking surgery underwent six cycles of adjuvant chemotherapy, and three (13%) underwent chemotherapy alone. All patients who underwent interval debulking surgery had complete macroscopic disease clearance.

Measurable disease was present in all 32 responders after the first cycle, in 26 (81%) after the third cycle, and in 10 (31%) at the end of treatment (Fig 1). Fourteen (44%) of 32 responders achieved the integrated response criteria after the first cycle, a further 17 (53%) after the third cycle, and one (3%) after the sixth cycle. Because of exclusion of lesions shrinking beyond measurability, evaluation was performed in 118 lesions (92 in responders, 26 in nonresponders) at baseline, 113 lesions (87 in responders, 26 in nonresponders) after the first cycle, and 81 lesions (55 in responders, 26 in nonresponders) after the third cycle. In no patient was nonresponse determined because of the appearance of a new lesion. Among 32 responders, 27



Table 1

## Patient Characteristics and Therapies

Characteristic	Datum
No. of patients	42
Histologic diagnosis (ovarian carcinoma)	31
Serous papillary adenocarcinoma	27
Poorly differentiated	23
Moderately differentiated	2
Well differentiated	2
Endometrioid adenocarcinoma	4
Poorly differentiated	1
Moderately differentiated	2
Well differentiated	1
Primary peritoneal carcinoma*	11
Disease status	
Primary	22
Recurrent	20
Current treatment	
Carboplatin and paclitaxel	25
Single agent carboplatin	6
Carboplatin and doxorubicin	5
Carboplatin and capecitabine	1
Carboplatin and phenoxodiol	2
Single agent paclitaxel	3
Total no. of evaluated lesions	118
No. of evaluated lesions per patient	
1	12
2	7
3	12
4	4
5	8
No. of evaluated lesions according to site	
Ovarian	13
Peritoneal	84
Omental	19
Visceral	2
Median pretreatment serum CA-125 level (IU/mL) <sup>†</sup>	502 (61–6236)

Note.—Unless otherwise indicated, data are numbers of patients.

\* All were poorly differentiated.

<sup>†</sup> Numbers in parentheses are ranges.

(84%) achieved 6-month progression-free survival, of whom 24 (89%) had no measurable residual disease and 22 (82%) had normal serum CA-125 level at the end of treatment.

### Reproducibility

Mean ADC from DW MR imaging repeated in 10 patients and 17 lesions (mean pixel count, 791; range, 120–2061) was calculated. For each lesion, the difference in mean ADC between the two series was expressed as percentage of the average ADC between the

series. There was no statistically significant difference ( $P = .80$ ) in mean ADC between the two series (series 1,  $1054 \times 10^{-6} \text{ mm}^2/\text{sec}$ ; series 2,  $1052 \times 10^{-6} \text{ mm}^2/\text{sec}$ ). Bland-Altman analysis yielded a coefficient of variation of 4.8%.

### Intra- and Interobserver Agreement

Among the randomly sampled lesions, three were excluded because of presence of artifact, which left 51 analyzable lesions. Intraclass correlation coefficients were 0.93 (95% confidence interval: 0.87, 0.96) and 0.86 (95%

confidence interval: 0.52, 0.94) for intra- and interobserver comparisons, respectively. Coefficients of intra- and interobserver variability were 11.4% and 13.7%, respectively.

### ADC Histogram Assessment

Median whole disease volume at baseline (calculated as the product of cumulative voxel count of target lesions at DW MR imaging and a nominal voxel volume of  $45 \text{ mm}^3$ ) was  $209.2 \times 10^3 \text{ mm}^3$  (range,  $3.8\text{--}2947.0 \times 10^3 \text{ mm}^3$ ) and did not differ significantly according to histologic grade ( $P = .69$ ), primary or recurrent disease status ( $P = .56$ ), and response outcome ( $P = .26$ ). Absolute mean percentage change in whole disease volume did not differ significantly between responders and nonresponders after the first cycle ( $-21.3\% \pm 33.3$  vs  $-6.1\% \pm 16.5$ , respectively,  $P = .06$ ) but was significantly higher in responders after the third cycle ( $-61.4\% \pm 34.7$  vs  $-22.8\% \pm 27.3$ , respectively,  $P = .003$ ). Absolute mean percentage change in CA-125 level was higher in responders than in nonresponders after the first ( $-40.7\% \pm 29.9$  vs  $-1.8\% \pm 33.8$ , respectively,  $P = .001$ ) and third ( $-78.8\% \pm 16.1$  vs  $1.4\% \pm 67.3$ , respectively,  $P = .004$ ) cycle.

Tumor grade, disease, and response status did not significantly affect ADC histogram parameters at baseline ( $P \geq .12$  for all factors) (Table 2). Pairwise comparisons demonstrated a significant increase in all ADC parameters ( $P < .001$ ) after the first cycle in responding patients, apart from histogram skew and kurtosis, whereas in nonresponding patients, no parameter changed significantly ( $P \geq .09$ ). After the third cycle, responders maintained the significant increase in all ADC parameters ( $P < .001$ ), with a significant decrease in skew ( $P < .001$ ) and kurtosis ( $P = .006$ ) compared with baseline; in nonresponders, no parameter changed significantly ( $P \geq .51$ ) (Figs 2, 3). Mean width of ADC histograms did not change significantly between baseline and after the first cycle in responders ( $.57 \times 10^{-3} \text{ mm}^2/\text{sec} \pm .18$  vs  $.63 \times 10^{-3} \text{ mm}^2/\text{sec} \pm .27$ , respectively,  $P = .11$ ) or nonresponders ( $.64 \times 10^{-3} \text{ mm}^2/\text{sec} \pm .10$  vs

**Table 2**

**ADC Histogram Values in Responders and Nonresponders at Each Chemotherapy Time Point**

Parameter	Responders					Nonresponders				
	Baseline (n = 32)	After First Cycle (n = 32)	P Value	After Third Cycle (n = 26)	P Value	Baseline (n = 10)	After First Cycle (n = 10)	P Value	After Third Cycle (n = 10)	P Value
Mean ADC ( $\times 10^{-3}$ mm <sup>2</sup> /sec)	1.08 $\pm$ 0.18	1.22 $\pm$ 0.22	<.001	1.30 $\pm$ 0.24	<.001	1.08 $\pm$ 0.15	1.11 $\pm$ 0.16	.26	1.12 $\pm$ .26	.55
10th percentile ( $\times 10^{-3}$ mm <sup>2</sup> /sec)	0.81 $\pm$ 0.15	0.94 $\pm$ 0.21	<.001	1.03 $\pm$ 0.21	<.001	0.80 $\pm$ 0.13	0.81 $\pm$ 0.13	.92	0.82 $\pm$ 0.19	.70
25th percentile ( $\times 10^{-3}$ mm <sup>2</sup> /sec)	0.91 $\pm$ 0.16	1.04 $\pm$ 0.21	<.001	1.14 $\pm$ 0.23	<.001	0.90 $\pm$ 0.14	0.90 $\pm$ 0.16	.83	0.93 $\pm$ 0.22	.65
50th percentile ( $\times 10^{-3}$ mm <sup>2</sup> /sec)	1.04 $\pm$ 0.19	1.18 $\pm$ 0.23	<.001	1.27 $\pm$ 0.26	<.001	1.04 $\pm$ 0.15	1.06 $\pm$ 0.17	.52	1.08 $\pm$ 0.27	.51
75th percentile ( $\times 10^{-3}$ mm <sup>2</sup> /sec)	1.21 $\pm$ 0.21	1.36 $\pm$ 0.25	<.001	1.43 $\pm$ 0.27	<.001	1.21 $\pm$ 0.17	1.27 $\pm$ 0.22	.09	1.26 $\pm$ 0.31	.51
90th percentile ( $\times 10^{-3}$ mm <sup>2</sup> /sec)	1.38 $\pm$ 0.24	1.56 $\pm$ 0.29	<.001	1.60 $\pm$ 0.30	<.001	1.44 $\pm$ 0.19	1.51 $\pm$ 0.24	.14	1.47 $\pm$ 0.35	.71
Skew	1.03 $\pm$ 0.64	0.95 $\pm$ 0.65	.53	0.58 $\pm$ 0.56	<.001	1.03 $\pm$ 0.51	0.98 $\pm$ 0.50	.71	1.11 $\pm$ 0.55	.66
Kurtosis	2.60 $\pm$ 3.66	2.09 $\pm$ 2.42	.45	0.63 $\pm$ 1.14	.006	1.77 $\pm$ 1.81	1.30 $\pm$ 1.66	.45	1.77 $\pm$ 2.03	.99

Note.—Data are interpatient means  $\pm$  standard deviations. P values refer to comparisons between pre- and posttreatment measurements in the responding and nonresponding groups.

**Figure 1**

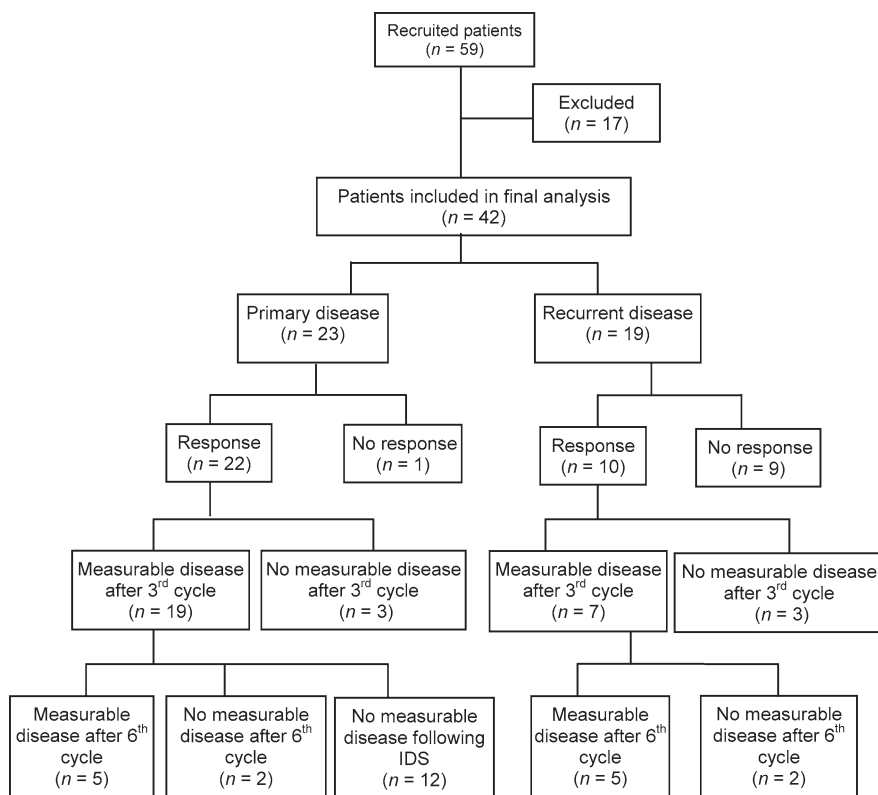


**Figure 1:** Flowchart of patient results. IDS = interval debulking surgery.

$.71 \times 10^{-3}$  mm<sup>2</sup>/sec  $\pm$  .22, respectively,  $P = .31$ ); no significant change was noted after the third cycle ( $P = .12$  and  $.88$  for responders and nonresponders, respectively).

Magnitude of change in ADC histogram parameters did not differ significantly according to tumor grade and disease status after the first ( $P \geq .08$  and  $.22$ , respectively) or after the third ( $P \geq .16$  and  $.21$ , respectively) cycle. The best discriminant parameter of response after both the first and third cycles was percentage change of the 25th percentile (% $\Delta$ C25) (AUC = 0.82 and 0.83, respectively), which was significantly higher in responders than in nonresponders but with considerable overlap (Table 3, Fig 4). However, its performance was not significantly superior to the percentage change of mean ADC (% $\Delta$ ADC<sub>mean</sub>) ( $P = .90$  and  $.87$  after first and third cycle, respectively). Application of linear discriminant analysis to all eight parameters (AUC<sub>all</sub>) and to the best combination at each time point did not improve accuracy (after first cycle: AUC<sub>all</sub> = 0.67, AUC<sub>% $\Delta$ C25+% $\Delta$ ADC<sub>mean</sub></sub> = 0.77; after third cycle: AUC<sub>all</sub> = 0.72, AUC<sub>% $\Delta$ C25+% $\Delta$ ADC<sub>mean</sub></sub> = 0.78). Highest accuracy was achieved with a cutoff value of 5.3% increase in percentage change

Figure 2

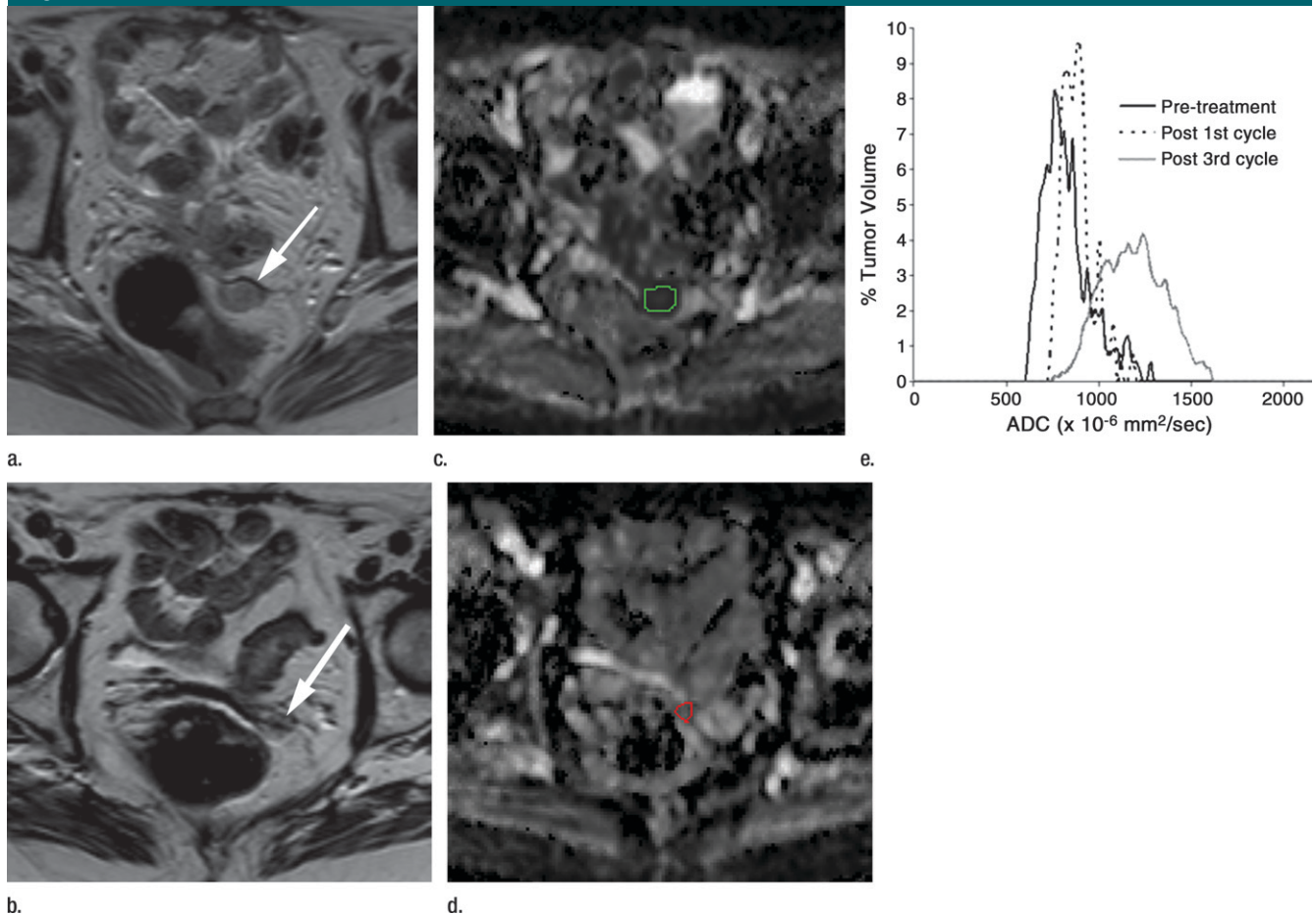


**Figure 2:** (a–e) Data in 69-year-old woman with single-site recurrent serous adenocarcinoma of the ovary. (a) Pretreatment axial T2-weighted MR image (echo time msec/repetition time msec, 84/5530) shows peritoneal metastasis in the left vaginal vault (arrow), measuring 21 mm in maximum diameter. After the first cycle of chemotherapy, no significant size change was evident (images not shown), but serum CA-125 level had decreased from 214 to 98 IU/mL (54.2% reduction). (b) After the third cycle, axial T2-weighted MR image (84/5530) shows the nodule (arrow) at 12 mm (43.8% size reduction), and corresponding CA-125 level was 21 IU/mL (90.2% reduction). (c) Pretreatment and (d) after-third-cycle axial ADC maps show ROIs generated with computer-assisted segmentation for ADC calculation. (e) Graph shows ADC histograms before treatment and after the first and third cycles, normalized for tumor volume. There is a continuing shift of the histograms to the right and a reduction in skewness. Mean ADC increased by 5.0% after the first cycle and by 42.4% after the third compared with baseline. The parameter with the highest percentage change after the first cycle was the 10th percentile (16.5% increase) and that after the third cycle was the 50th percentile (48.2% increase).

of the 25th percentile after the first cycle, which had 78.1% sensitivity, 80.0% specificity, 92.6% positive predictive value, and 46.2% negative predictive value for identifying response; combined CA-125 level and RECIST criteria at this time point had 43.7% sensitivity, 100% specificity, 64.8% positive predictive value, and 35.7% negative predictive value. Applying a threshold of 9.4% increase in percentage change of the 25th percentile, in accordance with the 95% confidence interval of

reproducibility, to the 28 patients whose response status was inconclusive according to conventional criteria after the first cycle would have resulted in additional correct classification of 10 of 18 subsequent responders and eight of 10 non-responders, achieving a positive predictive value of 89.8% with a negative predictive value of 36.0%.

There was a moderate inverse correlation between percentage change of disease volume (calculated from total voxel count) and percentage change of mean

ADC, percentage change of the 10th percentile, percentage change of the 25th percentile, and percentage change of the 50th percentile after the first cycle; after the third cycle, the relationship was stronger for all ADC parameters (with a positive correlation for change in skew and kurtosis) (Table 4). There was a moderate inverse correlation of similar magnitude between percentage change in all ADC parameters (apart from skew and kurtosis) and CA-125 level at both intratreatment time points.

**Figure 3**

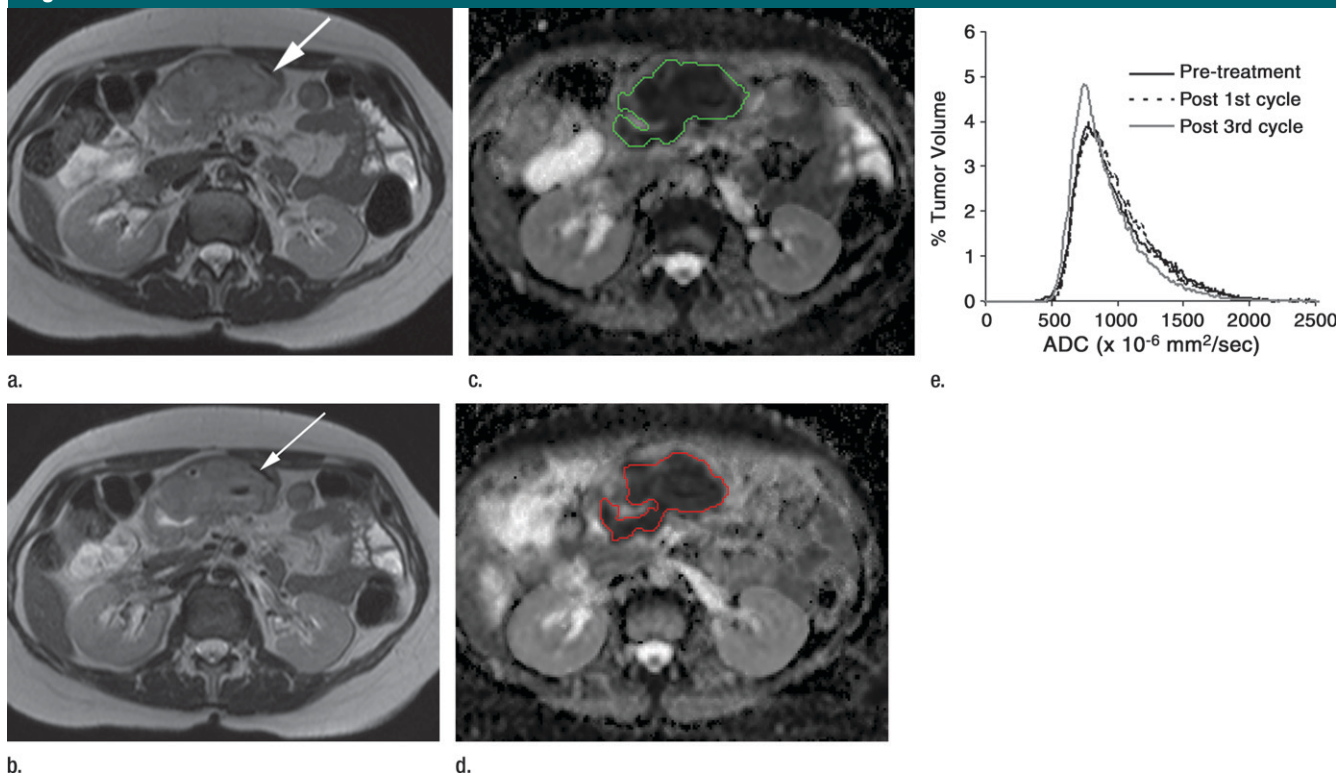


**Figure 3:** (a–e) Data in 56-year-old woman with multisite relapsed serous adenocarcinoma of the ovary. (a) Pretreatment axial T2-weighted MR image (84/5530) shows peritoneal metastasis in the gastric pylorus (arrow), measuring 81 mm. Other target lesions were located in the porta hepatis, falciform ligament, and rectosigmoid. After the first cycle of chemotherapy, no significant size change was evident and CA-125 level had decreased from 502 to 475 IU/mL (5.4% reduction). (b) After the third cycle, axial T2-weighted MR image (84/5530) shows the mass (arrow) at 82 mm, while the sum of maximum diameters of all target lesions had decreased from 278 to 254 mm (8.6% size reduction) and CA-125 level was 310 IU/mL (38.2% reduction), indicating nonresponse. (c) Pretreatment and (d) after-third-cycle axial ADC maps show ROIs generated with computer-assisted segmentation for ADC calculation. (e) Graph shows cumulative ADC histograms from target lesions before treatment and after the first and third cycles, normalized for tumor volume. The shape and location of the histogram curves are similar between the time points. Mean ADC increased by 0.4% after the first cycle and decreased by 7.3% after the third compared with baseline. Greatest percentage change after the first cycle was 2.5% reduction for the 90th percentile and that after the third cycle was 9.6% reduction for the 75th percentile.

**Table 3**

**Average Change of Total ADC Histogram Values in Responders and Nonresponders at Each Chemotherapy Time Point**

Parameter	Before to After First Cycle				Before to After Third Cycle			
	Responders (n = 32)	Nonresponders (n = 10)	PValue	AUC	Responders (n = 26)	Nonresponders (n = 10)	PValue	AUC
<b>Percentage change</b>								
Mean ADC	13.5 ± 12.6	2.8 ± 7.3	.022	0.80	22.8 ± 18.7	2.6 ± 15.7	.005	0.81
10th percentile	16.7 ± 20.0	1.5 ± 15.3	.098	0.78	27.4 ± 27.6	2.4 ± 16.9	.013	0.79
25th percentile	14.4 ± 15.4	-9.8 ± 30.5	.008	0.82	26.7 ± 24.3	-5.7 ± 31.8	.004	0.83
50th percentile	13.7 ± 13.6	2.8 ± 7.3	.021	0.78	25.3 ± 21.7	3.3 ± 17.1	.007	0.79
75th percentile	12.8 ± 12.6	4.6 ± 8.1	.054	0.73	22.1 ± 17.4	3.0 ± 16.0	.004	0.79
90th percentile	13.8 ± 16.5	5.0 ± 10.4	.159	0.67	19.7 ± 17.0	1.1 ± 16.0	.010	0.81
<b>Change</b>								
Skew	-0.08 ± 0.68	-0.05 ± 0.44	.595	0.46	-0.54 ± 0.66	0.11 ± 0.48	.010	0.80
Kurtosis	-0.51 ± 3.75	-0.47 ± 1.86	.973	0.48	-2.42 ± 4.08	-0.01 ± 1.96	.083	0.74

Note.—Data are interpatient means ± standard deviations. AUC is for discrimination of responders from nonresponders.



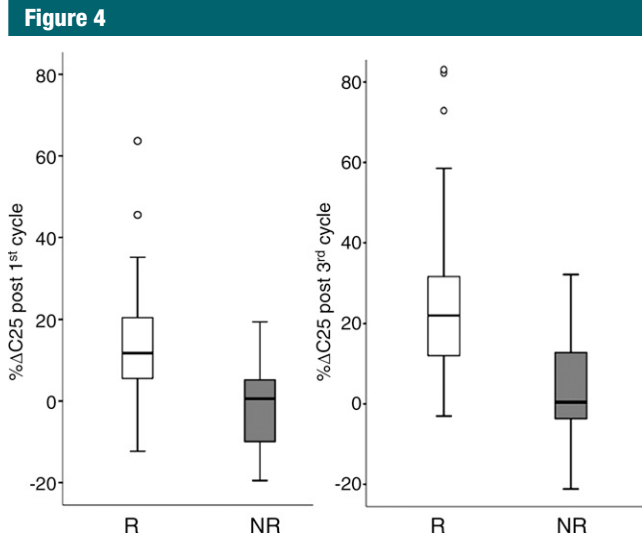


**Figure 4:** Box plots compare percentage change of 25th percentile ( $\% \Delta C25$ ) after the first and third cycle of chemotherapy between responders (*R*) and nonresponders (*NR*). Medians (lines through boxes) are higher in responders than in nonresponders, although there is considerable overlap.  $\circ$  = outliers.

### Progression-Free Survival

Absence of measurable disease (hazard ratio of 0.01,  $P = .039$ ) and normalization of serum CA-125 level (hazard ratio of 0.31,  $P = .046$ ) at the end of treatment were significant predictors of 6-month progression-free survival, whereas age, tumor grade, disease status, and percentage change of the 25th percentile after the first cycle were not significant (Table 5).

### Discussion

We have shown that ADC histogram parameters have predictive value in assessing chemotherapy response defined with integrated biochemical and morphologic criteria, irrespective of histologic grade and primary versus relapsed disease status. Response was associated with an early and sustained increase of ADCs and a later decrease of skew and kurtosis on cumulative histograms, reflecting total disease burden. Visually, these diffusivity changes translated into a shift of the histograms toward the right and adoption of a more symmetrical shape, respectively. Lack of response was associated with stability of all histogram parameters. The parameter with the highest accuracy in identifying responders was percentage

change of the 25th percentile, suggesting that, within tumor, the domains of lower diffusivity may be more sensitive to cytotoxic processes. This is supported by the established inverse correlation between ADC and cell density, which implies that, in heterogeneous tumors, regions of lower ADC are more representative of grade and biologic behavior because of their increased cellular concentration (21–23). Interestingly, the combination of best discriminatory parameters did not improve accuracy; a similar lack of improvement in the extended model compared with individual components has been previously observed in brain tumors and attributed to the high intracorrelation of ADC histogram parameters (24). Our results indicated that computation of percentage change of the 25th percentile is sufficiently representative of ADC histogram evolution to obviate complex algorithms. However, in early assessment of treatment response, percentage change of the 25th percentile can improve the positive predictive value of conventional CA-125 level and RECIST criteria but not their negative predictive value, which is required for timely identification of nonresponders.

The histogram analysis approach has been applied in other tumors, where

DW MR imaging has been used to quantify water mobility changes before macroscopic tumor shrinkage. Pixel-by-pixel ADC histograms through the entire tumor volume capture different microenvironments of diffusivity, which may be masked by mean ADC analysis. Tozer et al (24) demonstrated that percentiles below the 50th percentile, histogram mode, and skew were discriminant between astrocytomas and oligodendrogliomas. Pope et al (10) calculated separate mean ADCs for the lower and higher components of bimodal ADC histograms in glioblastoma multiforme and found that tumors with lesser opposed to greater ADCs of the lower curve had reduced progression-free survival. Nowosielski et al (25) showed that increasing skew in ADC histograms of patients with recurrent high-grade glioma predicted reduced progression-free survival compared with stable or decreasing skew. Outside the brain, the use of ADC histogram analysis to monitor chemotherapy effects is not widely used, and this study illustrated its potential.

The 4.8% coefficient of reproducibility in our replicate ADC measurements indicated that changes greater than 9.5% (95% confidence interval) can be attributed with 95% probability to an underlying biologic process rather than physiologic or hardware variability.

Percentage change in ADC histogram parameters was higher in responders than nonresponders, which is in agreement with results from breast (26) and rectal (27) cancer. However, the magnitude of change had substantial variation, which did not appear to depend on histologic grade or disease status.

We found a significant inverse correlation between ADC change and established response biomarkers, which was higher for volume change and for the later intratreatment time point. Correlations of similar magnitude have been reported in liver (7) and cervical (8) tumors, indicating that a decline in disease activity can be inferred from rising ADCs. However, the moderate strength of correlation suggests that

Table 4

## Correlation between Change in Histogram Parameters and Percentage Change of Morphologic and Biochemical Biomarkers

Histogram Parameter	After First Cycle		After Third Cycle	
	Percentage Change of Tumor Burden Volume	Percentage Change of CA-125 Level	Percentage Change of Tumor Burden Volume	Percentage Change of CA-125 Level
<b>Percentage change</b>				
Mean ADC	-0.35 (.020)	-0.41 (.007)	-0.50 (.002)	-0.40 (.017)
10th percentile	-0.37 (.017)	-0.34 (.029)	-0.49 (0.003)	-0.39 (.018)
25th percentile	-0.37 (.015)	-0.40 (.010)	-0.57 (<.001)	-0.45 (.006)
50th percentile	-0.30 (.048)	-0.41 (.007)	-0.48 (.003)	-0.38 (.023)
75th percentile	-0.19 (.226)	-0.39 (.011)	-0.46 (.005)	-0.36 (.034)
90th percentile	-0.15 (.361)	-0.32 (.041)	-0.45 (.006)	-0.33 (.047)
<b>Change</b>				
Skew	0.02 (.883)	0.14 (.379)	0.51 (.002)	-0.29 (.087)
Kurtosis	0.24 (.126)	0.20 (.199)	0.52 (.002)	0.25 (.139)

Note.—Data are Spearman rank correlation coefficients, with *P* values in parentheses. Percentage change of tumor burden volume was calculated from summated voxel counts from all target lesions.

Table 5

## Multivariate Cox Regression Analysis for 6-Month Progression in Responders

Variable	Regression Coefficient	Standard Error	Hazard Ratio	<i>P</i> Value	95% Confidence Interval
Age	0.06	0.09	1.06	.488	0.89, 1.27
Tumor grade	0.60	1.85	1.83	.746	0.05, 69.00
Normal CA-125 level	-3.49	1.75	0.31	.046	0.00, 0.94
Absence of measurable residual disease	-4.29	2.07	0.01	.039	0.00, 0.80
Percentage change of 25th percentile	-0.11	0.07	0.90	.120	0.78, 1.27

Note.—Normal CA-125 level and absence of measurable residual disease refer to the end of treatment. Percentage change of 25th percentile refers to after the first cycle.

diffusivity changes reflect a multitude of structural and functional processes during treatment.

Baseline diffusivity parameters were not shown to be predictive of morphologic and biochemical response. The association between high pretreatment ADCs and unfavorable response reported in hepatic (7,28), breast (26), and rectal tumors (29) may not apply to all tumor types, as it has not been confirmed in cervical (8) and head and neck cancer (30).

As best ADC discriminant, percentage change of the 25th percentile did not appear to be predictive of 6-month progression-free survival. In central nervous system tumors, low pretreatment ADCs have been reported as independent risk factors of reduced survival (9,10,23,31). In comparison, advanced ovarian cancer is an intrinsically heterogeneous disease, as adnexal lesions

coexist at presentation with peritoneal and omental metastases, all of which have unique histologic features. The failure of ADC parameters to predict clinical outcome may in part arise from the endogenous diversity of lesions composing total disease burden. Furthermore, the small number of initial responders who experienced relapse and the relatively short observation period may have obscured any association of ADC change with clinical outcome.

Our study had limitations. First, we generated cumulative ADC histograms, weighted for individual lesion volume and corresponding to whole disease burden. The inherent disadvantage of this method was the inability to quantify within-patient and between-lesion variability and thus to address differential response. Second, the small number of nonresponders was not sufficient for the evaluation of multiparametric

regression models comprising CA-125 level, size, and ADC change, which would be of clinical relevance. Third, despite the prospective nature of the study, there was inevitable variation in the temporal window between chemotherapy administration and imaging, which may have contributed to the dispersion of ADC changes, because diffusivity patterns have been shown to be in part time-dependent (29). Fourth, concentrating on the five largest lesions may have introduced selection bias. Fifth, only short-term reproducibility of ADC measurements was assessed. Finally, lesions that shrunk to subcentimeter size were not analyzed further because of spatial resolution limitations. This may have led to overrepresentation of less-responsive lesions on the weighted ADC histograms.

In conclusion, ADC histogram analysis may be a useful adjunct tool to

conventional biomarkers for monitoring chemotherapeutic efficacy in advanced ovarian or primary peritoneal cancer. Our results indicated that an early and sustained increase of ADC mean and percentiles and later decrease of histogram skew and kurtosis can detect response assessed with integrated morphologic and biochemical criteria. The ability of DW MR imaging and ADC histograms to characterize different diffusion microenvironments can be used to quantify disease heterogeneity and potentially use the information to refine monitoring of treatment response.

**Acknowledgments:** We thank V. Morgan, MSc, for technical assistance with patient acquisitions. We also acknowledge T. Feiweier, PhD, (Siemens Healthcare Sector) for developing the WIP Diffusion package.

**Disclosures of Potential Conflicts of Interest:** **S.K.** No potential conflicts of interest to disclose. **D.J.C.** No potential conflicts of interest to disclose. **C.M.** No potential conflicts of interest to disclose. **K.P.** No potential conflicts of interest to disclose. **R.L.D.** No potential conflicts of interest to disclose. **S.L.G.** No potential conflicts of interest to disclose. **S.B.K.** No potential conflicts of interest to disclose. **N.M.d.S.** No potential conflicts of interest to disclose.

## References

- Jemal A, Siegel R, Xu J, Ward E. Cancer statistics, 2010. *CA Cancer J Clin* 2010;60(5):277–300.
- Ozols RF, Bundy BN, Greer BE, et al. Phase III trial of carboplatin and paclitaxel compared with cisplatin and paclitaxel in patients with optimally resected stage III ovarian cancer: a Gynecologic Oncology Group study. *J Clin Oncol* 2003;21(17):3194–3200.
- Greenlee RT, Hill-Harmon MB, Murray T, Thun M. Cancer statistics, 2001. *CA Cancer J Clin* 2001;51(1):15–36.
- Oaknin A, Barretina P, Pérez X, et al. CA-125 response patterns in patients with recurrent ovarian cancer treated with pegylated liposomal doxorubicin (PLD). *Int J Gynecol Cancer* 2010;20(1):87–91.
- Ferrandina G, Ludovisi M, Corrado G, Carone V, Petrillo M, Scambia G. Prognostic role of Ca125 response criteria and RECIST criteria: analysis of results from the MITO-3 phase III trial of gemcitabine versus pegylated liposomal doxorubicin in recurrent ovarian cancer. *Gynecol Oncol* 2008;109(2):187–193.
- Chen CY, Li CW, Kuo YT, et al. Early response of hepatocellular carcinoma to transcatheter arterial chemoembolization: choline levels and MR diffusion constants—initial experience. *Radiology* 2006;239(2):448–456.
- Cui Y, Zhang XP, Sun YS, Tang L, Shen L. Apparent diffusion coefficient: potential imaging biomarker for prediction and early detection of response to chemotherapy in hepatic metastases. *Radiology* 2008;248(3):894–900.
- Harry VN, Semple SI, Gilbert FJ, Parkin DE. Diffusion-weighted magnetic resonance imaging in the early detection of response to chemoradiation in cervical cancer. *Gynecol Oncol* 2008;111(2):213–220.
- Barajas RF Jr, Rubenstein JL, Chang JS, Hwang J, Cha S. Diffusion-weighted MR imaging derived apparent diffusion coefficient is predictive of clinical outcome in primary central nervous system lymphoma. *AJNR Am J Neuroradiol* 2010;31(1):60–66.
- Pope WB, Kim HJ, Huo J, et al. Recurrent glioblastoma multiforme: ADC histogram analysis predicts response to bevacizumab treatment. *Radiology* 2009;252(1):182–189.
- Low RN, Sebrechts CP, Barone RM, Muller W. Diffusion-weighted MRI of peritoneal tumors: comparison with conventional MRI and surgical and histopathologic findings—a feasibility study. *AJR Am J Roentgenol* 2009;193(2):461–470.
- Sala E, Priest AN, Kataoka M, et al. Apparent diffusion coefficient and vascular signal fraction measurements with magnetic resonance imaging: feasibility in metastatic ovarian cancer at 3 Tesla—technical development. *Eur Radiol* 2010;20(2):491–496.
- Yap TA, Carden CP, Kaye SB. Beyond chemotherapy: targeted therapies in ovarian cancer. *Nat Rev Cancer* 2009;9(3):167–181.
- Baek SJ, Park JY, Kim DY, et al. Stage IIIC epithelial ovarian cancer classified solely by lymph node metastasis has a more favorable prognosis than other types of stage IIIC epithelial ovarian cancer. *J Gynecol Oncol* 2008;19(4):223–228.
- Braithwaite AC, Dale BM, Boll DT, Merkle EM. Short- and midterm reproducibility of apparent diffusion coefficient measurements at 3.0-T diffusion-weighted imaging of the abdomen. *Radiology* 2009;250(2):459–465.
- Rustin GJ, Vergote I, Eisenhauer E, et al. Definitions for response and progression in ovarian cancer clinical trials incorporating RECIST 1.1 and CA 125 agreed by the Gynecological Cancer Intergroup (GCIIG). *Int J Gynecol Cancer* 2011;21(2):419–423.
- Eisenhauer EA, Therasse P, Bogaerts J, et al. New response evaluation criteria in solid tumours: revised RECIST guideline (version 1.1). *Eur J Cancer* 2009;45(2):228–247.
- Bland JM, Altman DG. Measuring agreement in method comparison studies. *Stat Methods Med Res* 1999;8(2):135–160.
- Shrout PE, Fleiss JL. Intraclass correlations: uses in assessing rater reliability. *Psychol Bull* 1979;86(2):420–428.
- Johnson RA, Wichern DW. Applied multivariate statistical analysis. 5th ed. Englewood Cliffs, NJ: Prentice Hall, 2002.
- Sugahara T, Korogi Y, Kochi M, et al. Usefulness of diffusion-weighted MRI with echoplanar technique in the evaluation of cellularity in gliomas. *J Magn Reson Imaging* 1999;9(1):53–60.
- Guo AC, Cummings TJ, Dash RC, Provenzale JM. Lymphomas and high-grade astrocytomas: comparison of water diffusibility and histologic characteristics. *Radiology* 2002;224(1):177–183.
- Higano S, Yun X, Kumabe T, et al. Malignant astrocytic tumors: clinical importance of apparent diffusion coefficient in prediction of grade and prognosis. *Radiology* 2006;241(3):839–846.
- Tozer DJ, Jäger HR, Danchaivijitr N, et al. Apparent diffusion coefficient histograms may predict low-grade glioma subtype. *NMR Biomed* 2007;20(1):49–57.
- Nowosielski M, Recheis W, Goebel G, et al. ADC histograms predict response to antiangiogenic therapy in patients with recurrent high-grade glioma. *Neuroradiology* 2011;53(4):291–302.
- Park SH, Moon WK, Cho N, et al. Diffusion-weighted MR imaging: pretreatment prediction of response to neoadjuvant chemotherapy in patients with breast cancer. *Radiology* 2010;257(1):56–63.
- Sun YS, Zhang XP, Tang L, et al. Locally advanced rectal carcinoma treated with preoperative chemotherapy and radiation therapy: preliminary analysis of diffusion-weighted MR imaging for early detection of tumor histopathologic downstaging. *Radiology* 2010;254(1):170–178.
- Koh DM, Scurr E, Collins D, et al. Predicting response of colorectal hepatic metastasis: value of pretreatment apparent diffusion coefficients. *AJR Am J Roentgenol* 2007;188(4):1001–1008.
- Dzik-Jurasz A, Domenig C, George M, et al. Diffusion MRI for prediction of response of rectal cancer to chemoradiation. *Lancet* 2002;360(9329):307–308.
- King AD, Mo FK, Yu KH, et al. Squamous cell carcinoma of the head and neck: diffusion-weighted MR imaging for prediction and monitoring of treatment response. *Eur Radiol* 2010;20(9):2213–2220.
- Oh J, Henry RG, Pirzkall A, et al. Survival analysis in patients with glioblastoma multiforme: predictive value of choline-to-N-acetylaspartate index, apparent diffusion coefficient, and relative cerebral blood volume. *J Magn Reson Imaging* 2004;19(5):546–554.